Appl Microbiol Biotechnol (2016) 100:10395–10402
DOI 10.1007/s00253-016-7689-z

α-Galactosidase delivery using 30Kc19-human serum albumin nanoparticles for effective treatment of Fabry disease

Hong Jai Lee[1] · Hee Ho Park[1] · Youngsoo Sohn[2] · Jina Ryu[2] · Ju Hyun Park[3] · Won Jong Rhee[4] · Tai Hyun Park[1,2,5]

Received: 19 April 2016 / Revised: 12 June 2016 / Accepted: 14 June 2016 / Published online: 29 June 2016

Abstract Fabry disease is a genetic lysosomal storage disease caused by deficiency of α-galactosidase, the enzyme-degrading neutral glycosphingolipid that is transported to lysosome. Glycosphingolipid accumulation by this disease causes multi-organ dysfunction and premature death of the patient. Currently, enzyme replacement therapy (ERT) using recombinant α-galactosidase is the only treatment available for Fabry disease. To maximize the efficacy of treatment, enhancement of cellular delivery and enzyme stability is a challenge in ERT using α-galactosidase. In this study, protein nanoparticles using human serum albumin (HSA) and 30Kc19 protein, originating from silkworm, were used to enhance the delivery and intracellular α-galactosidase stability. 30Kc19-HSA nanoparticles loaded with the α-galactosidase were formed by desolvation method. 30Kc19-HSA nanoparticles had a uniform spherical shape and were well dispersed in cell culture media. 30Kc19-HSA nanoparticles had negligible toxicity to human cells. The nanoparticles exhibited enhanced cellular uptake and intracellular stability of delivered α-galactosidase in human foreskin fibroblast. Additionally, they showed enhanced globotriaosylceramide degradation in Fabry patients' fibroblasts. It is expected that 30Kc19-HSA protein nanoparticles could be used as an effective tool for efficient delivery and enhanced stability of drugs.

Keywords Fabry disease · Enzyme replacement therapy · Protein nanoparticle · Drug delivery · Enzyme stability

Introduction

Fabry disease is a rare X-linked disorder of lysosomal storage caused by deficiency of α-galactosidase (Scriver 2001). Since α-galactosidase hydrolyzes neutral glycosphingolipids at lysosomes, lack of this enzyme results in accumulation of glycosphingolipids, mainly globotriaosylceramide (Gb3), in various tissues. It causes multi-organ dysfunction and premature death of the patient. Enzyme replacement therapy (ERT), administrating recombinant enzyme to patients, is the only treatment available for lysosomal disorder like Fabry disease (Lee et al. 2003). Commercial recombinant human α-galactosidase (e.g., Fabrazyme) is used for ERT of Fabry disease. However, administrated α-galactosidase has shown vulnerability to clearance from blood by the liver and kidney and degradation by proteases and immune reaction in vivo (Linthorst et al. 2004). Furthermore, since cost of commercial α-galactosidase for ERT is very high, appropriate drug delivery system for effective treatment of Fabry disease is required (Vedder et al. 2007).

Diverse nanoparticles are applied to drug delivery since nanocarriers can protect cargos from degradation and enhance intracellular penetration (Wang et al. 2008). Among various nanoparticles, polymeric nanoparticles have additional advantage in protecting their therapeutic cargos located inside. Protein is a

Hong Jai Lee and Hee Ho Park are the co-first authors in this study.

✉ Tai Hyun Park
thpark@snu.ac.kr

[1] The School of Chemical and Biological Engineering, Seoul National University, 1 Gwanak-ro, Gwanak-gu, Seoul, Republic of Korea

[2] Interdisciplinary Program for Bioengineering, Seoul National University, Seoul, Republic of Korea

[3] Department of Medical Biomaterials Engineering, Kangwon National University, Chuncheon, Republic of Korea

[4] Division of Bioengineering, Incheon National University, Academy-ro, Yeonsu-gu, Incheon 406-772, Republic of Korea

[5] Advanced Institutes of Convergence Technology, Suwon, Republic of Korea

suitable polymeric material for nanocarriers since it has beneficial features such as non-toxicity and biodegradability (Kumar 2000).

Albumin is the most actively studied protein because it is a FDA-approved material for therapeutic use and has abundant functional groups to bind with cargos and can perform modification with ligands (Irache et al. 2005; Weber et al. 2000). Albumin has its own endocytosis route mediated by gp60; albumin receptor is located at caveolae. However, there are cells lacking or having limited caveolae, and in such cases, additional ligands are desirable to efficiently deliver albumin nanoparticles loaded with therapeutics into target cells. Maintaining activity of drug cargo is also challenging since enzyme cargo might be deactivated during nanoparticle preparation process and after intracellular delivery. Cell-penetrating peptides and various target-specific ligands are being applied to albumin nanoparticles to achieve enhanced delivery (Elzoghby et al. 2012; Irache et al. 2005; Zensi et al. 2009), but there are only few studies in enhancing stability of cargos, especially therapeutic enzyme. In this work, recombinant 30Kc19 protein originating from silkworm was used together with albumin to form nanoparticles in order to enhance both cellular uptake and cargo stability.

30Kc19 protein is a member of the 30K protein family found in silkworm hemolymph, having molecular weights around 30 kDa. In our previous studies, anti-apoptotic effect was observed in various cells via 30K gene expression or addition of 30K proteins in recombinant form produced from *Escherichia coli* (Choi et al. 2006; Choi et al. 2002; Choi et al. 2005; Ha and Park 1997; Ha et al. 1996; Kim et al. 2003; Kim and Park 2003; Kim et al. 2004; Park et al. 2015; Rhee et al. 1999; Rhee et al. 2002; Rhee and Park 2000; Wang et al. 2011). Moreover, in recent studies, cell-penetrating and enzyme-stabilizing effects of 30Kc19 protein were also observed (Park et al. 2014; Park et al. 2012a; Park et al. 2012b). Thus, the 30Kc19 protein is suitable to enhance cellular uptake and stabilizing activity of drug cargo; hence, 30Kc19 protein-human serum albumin (HSA) hybrid protein nanoparticles were synthesized. These 30Kc19-HSA nanoparticles exhibited cellular uptake and intracellular stability enhancement of model enzyme cargo (Lee et al. 2014). In this study, 30Kc19-HSA nanoparticles were used to deliver therapeutic enzyme and its beneficial effect was evaluated. The 30Kc19-HSA nanoparticles loaded with α-galactosidase, the therapeutic enzyme for treatment of Fabry disease, were prepared and characterized. Then, cellular uptake, intracellular enzyme cargo activity, and Gb3 degradation were examined using 30Kc19-HSA nanoparticles loaded with α-galactosidase.

Materials and methods

Production of 30Kc19 protein

30Kc19 protein was produced as described in our previous work (Park et al. 2012b). Briefly, the 30Kc19 gene was inserted into a pET-23a expression vector (Novagen, USA) with a T7 tag at the N-terminus and a 6× His tag at C-terminus, and 30Kc19 protein was produced using *30Kc19* vector-transformed *E. coli* BL21 (Novagen, USA). Cells were cultured in LB medium containing 100 μg/ml ampicillin at 37 °C and induced with isopropyl-α-D-thiogalactopyranoside (IPTG, 1 mM). Cells were harvested after further incubation for 4 h at 37 °C and then disrupted by ultrasonication. The 30Kc19 protein was purified from the supernatant using a HisTrap HP column (GE Healthcare, Sweden) and dialyzed with phosphate-buffered saline (PBS) using desalting column (GE Healthcare, Sweden). Final purity of 30Kc19 protein was higher than 90 % (data not shown). The purified 30Kc19 protein was stored at −70 °C. The quantity of 30Kc19 was assessed using a Micro BCA kit (Thermo Fisher Scientific Inc., USA).

Preparation of nanoparticles

HSA-30Kc19 protein nanoparticles were prepared by desolvation method as described previously (Park et al. 2012b). Human serum albumin (HSA, Sigma-Aldrich, Austria), 30Kc19 protein, and 80 μg of α-galactosidase (kindly provided by Isu Abxis, Korea) were dissolved to 500 μl of Tris-HCl buffer (pH 9.0). Total 1 mg of HSA and 30Kc19 was added with various ratios. Then, 2 ml of 100 % ethanol was added dropwise using a syringe pump under constant stirring (1000 rpm) at room temperature. Consequently, nanosized protein aggregate containing α-galactosidase was formed. Prepared 30Kc19-HSA nanoparticles containing α-galactosidase were further stabilized by 5 μl of 10 % glutaraldehyde aqueous solution for 40 min in room temperature. Nanoparticles were harvested by centrifugation (Sigma-Aldrich, Austria) at 12,000×*g*, 4 °C for 20 min. Protein nanoparticles were washed additionally with PBS buffer three times.

Size, polydispersity index, and zeta potential of nanoparticles

Particle size and zeta potential of the nanoparticles were measured by electrophoretic light scattering spectrophotometer (ELS-8000, Otsuka, Japan). Before measurement, 1 mg/ml protein nanoparticles were centrifuged at 4 °C, 12,000 rpm for 10 min, and resuspended 1/10 (*v*/*v*) with deionized water. Samples were then transferred into a quartz cuvette in an ELS-8000 dynamic light scattering instrument. Size and zeta potential of nanoparticles were determined using corresponding mode of electrophoretic light scattering (ELS) spectrometer according to the manufacturer's instruction.

SEM analysis of nanoparticles

Scanning electron microscopy (SEM) analysis was performed to visualize the morphology of protein nanoparticles. Prepared

protein nanoparticle sample was diluted 1/10 (*v*/*v*) with deionized water. Ten-microliter drop of nanoparticle in aqueous solution was placed on 12-mm circular coverslip and lyophilized using a freeze dryer (Hanil, Korea). Each dried sample with the coverslip was placed on a stub using a carbon tape and sputter-coated with Pt, and SEM image was obtained using field emission scanning electron microscope (FE-SEM, JSM-6700F, JEOL, Japan). The acceleration voltage was 2.0 kV and the magnification was ×50,000.

Loading efficiency of α-galactosidase in nanoparticles

30Kc19-HSA nanoparticles were prepared using Alexa Fluor® 488-labeled α-galactosidase to assess α-galactosidase loading. To do this, α-galactosidase was labeled with green fluorescent Alexa Flour® 488, using protein labeling kit (Invitrogen, USA) according to the manufacturer's instruction. Briefly, 1 mg/ml α-galactosidase, Alexa Fluor® 488, and sodium bicarbonate buffer (pH 8.3) were mixed for 20 min by rocking at room temperature. After preparation, the nanoparticle solution was centrifuged at 4 °C, 12,000 rpm for 10 min using a Vivaspin® 500 ultrafiltration spin column (Sartorius, Hannover, Germany). Any unbound flow through was discarded and repeated several times. Then, separated supernatant was collected. Fluorescence was measured with a spectrofluorometer (Tecan, Salzburg, Austria) with an excitation at 485 nm (20-nm bandwidth), emission at 535 nm (25-nm bandwidth), and gain of 60. Loading efficiency was determined indirectly by subtracting remaining α-galactosidase fluorescence in supernatant from initial one. Correlation curve between the fluorescence intensity of Alexa Fluor® 488 and the α-galactosidase concentration was prepared prior to this experiment.

Cell viability

To examine the cytotoxicity of 30K-HSA nanoparticles to cells, human foreskin fibroblasts were seeded on a 96-well plate at 70 % confluency, and nanoparticles in DMEM (4 μg/ml α-galactosidase content in media) were added to the well and incubated for 24 h in 37 °C, 5 % CO_2 incubator. Then, 3,(4,5-dimethylthiazol-2-yl)2,3-diphenyl-tetrazolium (MTT) was added to the media at 0.5 mg/ml and incubated for 2 h. Developed formazan crystal was solubilized using dimethyl sulfoxide (DMSO, Sigma-Aldrich, Austria), and absorbance was measured at 560 nm using the ELISA reader.

Cellular uptake of nanoparticles

To assess the cellular uptake of nanoparticles, human foreskin fibroblasts were seeded on a 96-well plate and incubated overnight. Alexa Fluor® 488-labeled nanoparticles in DMEM (4 μg/ml α-galactosidase content in media) were added to well and incubated for 12 h at 37 °C. After incubation, cells were washed with PBS, and fluorescence of cells was obtained using fluorometer (Tecan, Australia).

Cellular uptake of protein nanoparticles in cells was also visualized using confocal microscopy. Human foreskin fibroblast cells were seeded on an eight-well chamber plate and incubated overnight. Alexa Fluor® 488-labeled nanoparticles in DMEM (4 μg/ml α-galactosidase content in media) were added to well and incubated for 12 h at 37 °C. After nanoparticle incubation, the media were exchanged with DMEM supplemented with 10 % FBS, or 10 % FBS with LysoTracker (Sigma-Aldrich, Austria) for lysosome targeting, and further incubated for 1 h. Nanoparticle-treated cells were washed with PBS twice, fixed with 4 % paraformaldehyde for 20 min, and permeabilized with 0.25 % Triton X-100 in PBS. Nuclei of cells were stained with Hoechst 33342 for 10 min. Confocal laser microscope (EZ-C1, Nikon, Japan) was used to observe intracellular fluorescence, and image was taken by the manufacturer's software (Nikon, Japan).

Activity of α-galactosidase in nanoparticle-treated cells

The α-galactosidase activity in cells treated with nanoparticles was determined using colorimetric assay. To perform α-gal assay, human foreskin fibroblast cells were seeded on a 24-well plate at 70 % confluency, and nanoparticles in DMEM (4 μg/ml α-galactosidase content in media) were added to the well and incubated for 24 h in 37 °C, 5 % CO_2 incubator. After incubation, the media were exchanged with DMEM supplemented with 10 % FBS for 1 h. Cells were washed twice with PBS, and 100 μl of RIPA buffer was added to the well to obtain cell lysate. After 10 min of incubation at room temperature, 10 μl of cell lysate was placed to a 96-well plate and α-gal assay was performed as described earlier.

Globotriaosylceramide degradation in nanoparticle-treated cells

To examine intracellular globotriaosylceramide (Gb3) degradation activity in nanoparticle-treated cells, Fabry disease patients' fibroblasts (Coriell Institute for Medical Research, NJ, USA) were seeded on a 96-well plate and incubated overnight. *N*-dodecanoyl-NBD-ceramide trihexoside (NBD-Gb3, Abcam, USA), a green fluorescent Gb3 analog, was added (2 μg/ml in media) and incubated overnight. Then, nanoparticles in DMEM (4 μg/ml α-galactosidase content in media) were added to the well and incubated for 12 h at 37 °C. After incubation, the cells were washed with PBS. The remaining NBD-GB3 fluorescence of cells was measured using fluorometer (Tecan,

Australia), and Gb3 degradation was calculated indirectly by subtracting it from the initial NBD-GB3 fluorescence.

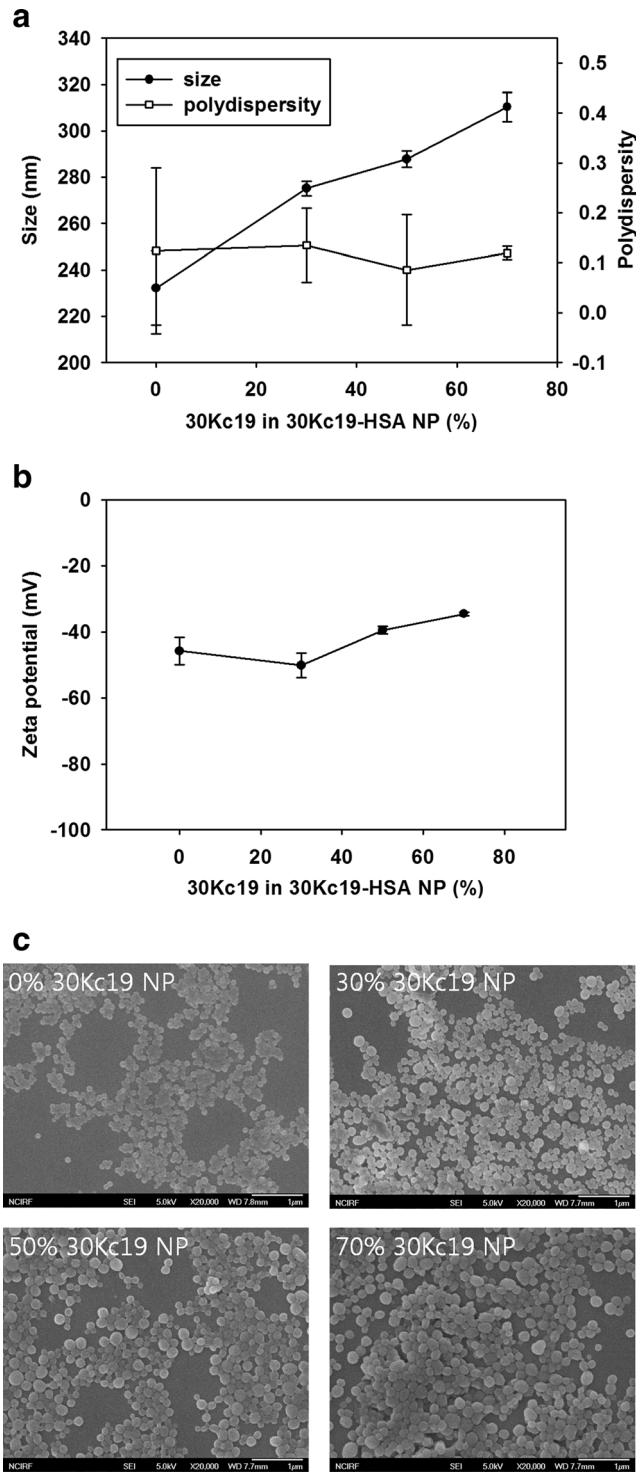

Fig. 1 Characterization of prepared 30Kc19-HSA nanoparticles. **a** Nanoparticle size and polydispersity versus weight percentage of 30Kc19 protein in nanoparticles. **b** Zeta potential of nanoparticles. **c** SEM images of 30Kc19-HSA nanoparticles containing 0–70 % of 30Kc19 protein (magnification ×20,000). *$p < 0.05$, compared with the control group ($n = 3$). *Error bars* represent standard deviation

Statistical analysis

All values were written as the mean ± S.D. All experiments were performed in triplicate and compared with the control using the *t* test. $p < 0.05$ was considered statistically significant.

Results

Production and characterization of 30Kc19-HSA nanoparticles

30Kc19-HSA protein nanoparticles were prepared by desolvation method (von Storp et al. 2012). Desolvation process involves dropwise addition of ethanol to aqueous solution containing HSA, 30Kc19 protein, and α-galactosidase. As the mixture dehydrates gradually by ethanol, protein molecules lose their stable hydrated conformation and aggregates with neighboring molecules. With appropriate condition, this aggregation occurs in a controlled uniform size. The aggregated protein

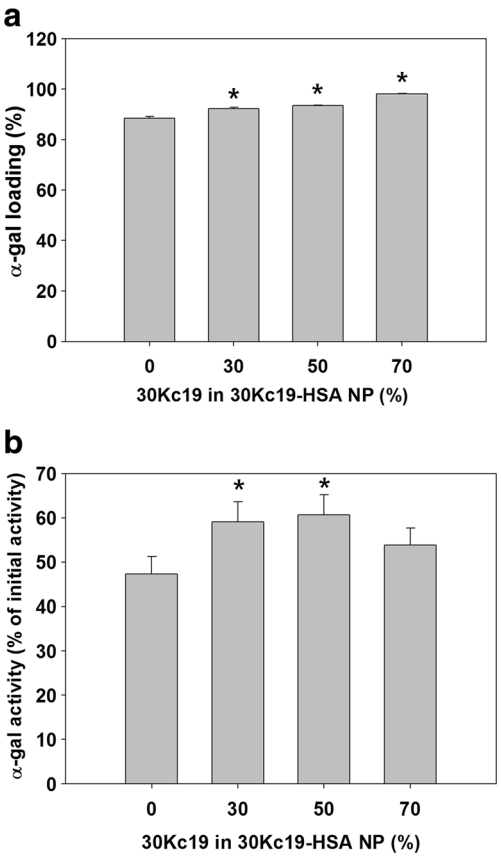

Fig. 2 Effect of 30Kc19 on enzyme loading efficiency and enzyme stabilization. **a** α-Galactosidase loading efficiency of 30Kc19-HSA nanoparticles with increasing wt% (0–70 %) of 30Kc19 protein, which was indirectly measured using fluorescent-labeled enzyme remaining in the supernatant of the reaction solution. **b** Activity of α-galactosidase loaded in 30Kc19-HSA nanoparticles, which was measured using α-galactosidase activity assay. *$p < 0.05$, compared with the control group ($n = 3$). *Error bars* represent standard deviation

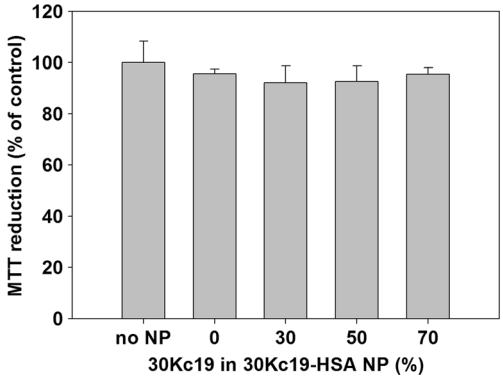

Fig. 3 MTT assay of human foreskin fibroblast cells treated with 200 μg/ml of 30Kc19-HSA nanoparticles containing 0–50 wt% of 30Kc19 protein for 24 h. Then, 0.5 mg/ml MTT was added to the media and incubated for 2 h. The formazan crystals that developed were solubilized with DMSO, and absorbance was measured at 560 nm using the ELISA reader. $p > 0.05$, compared with the control group ($n = 3$). *Error bars* represent standard deviation

nanoparticles are stabilized using crosslinking agent (e.g., glutaraldehyde) (Zensi et al. 2009). Then, size, polydispersity, and zeta potential of synthesized 30Kc19-HSA nanoparticles were measured using ELS spectrophotometry. The results showed that nanoparticle sizes increased with increasing weight percentage of 30Kc19 protein, from 230 nm 0 % 30Kc19 to 310 nm 70 % 30Kc19. Polydispersity index is a measure of size distribution of the nanoparticle population parameters, and it depends on parameters such as temperature, concentration, and desolvating agent for the synthesis of protein nanoparticles (Azarmi et al. 2006). Although fluctuation in standard deviations was observed, polydispersity of nanoparticles was about 0.1 regardless of the percentage of 30Kc19, indicating the uniform size of prepared nanoparticles (Fig. 1a). Zeta potential of 30Kc19-HSA nanoparticles was ~−40 mV at neutral pH (Fig. 1b), corresponding with stable dispersion of nanoparticles observed in water, PBS, and cell culture media. SEM image was obtained to evaluate the effect of 30Kc19 protein on morphology of nanoparticles (Fig. 1c). Uniform spherical shape was observed in all wt% of 30Kc19 nanoparticles.

Loading efficiency of α-galactosidase was assessed indirectly using fluorescent-labeled enzyme remaining in the supernatant of the reaction solution (Fig. 2a). The α-galactosidase was loaded to the nanoparticle with high yield, 80–95 %. The enzyme loading increased very little with the wt% of 30Kc19 in nanoparticles. Enzyme activity of nanoparticles containing α-galactosidase was measured using colorimetric assay (Fig. 2b). Specific activity of α-galactosidase inside nanoparticles increased by more than 20 % with 30 and 50 wt% of 30Kc19. However, it is noticeable that the α-galactosidase activity was lowered in 70 wt% 30Kc19 nanoparticles and negligible difference was observed compared with the control.

Cellular toxicity of 30Kc19-HSA nanoparticle containing α-galactosidase was measured using MTT assay (Fig. 3). In this study, human foreskin fibroblast was chosen as target delivery cell since target of α-galactosidase would be human primary cells. No significant decrease in the MTT reduction was observed in human foreskin fibroblast for 0–70 % 30Kc19 in nanoparticles. Therefore, treatment of 30Kc19-HSA nanoparticles exhibited no toxicity on human primary cells.

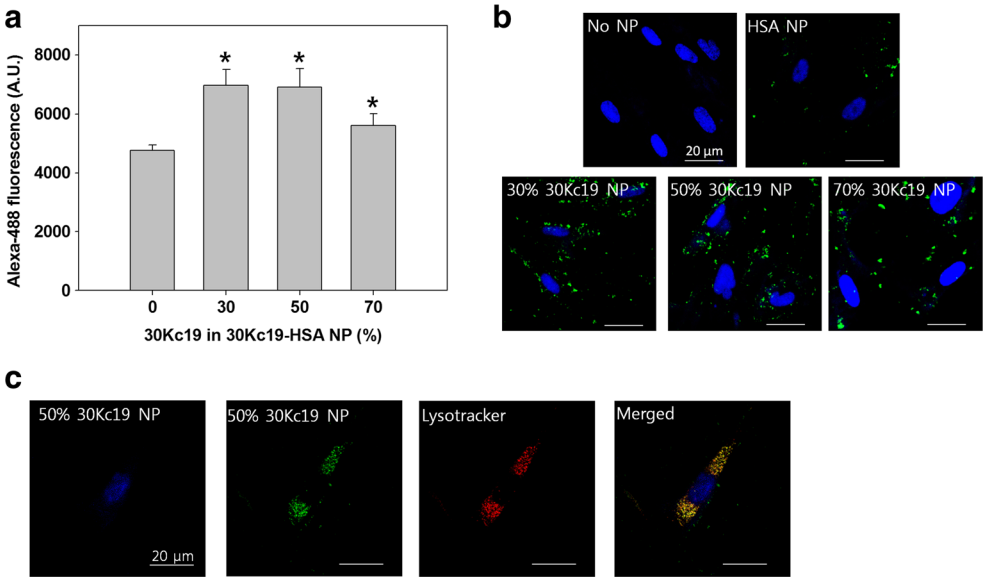

Fig. 4 Cellular uptake of 30Kc19-HSA nanoparticles. **a** Quantitative cellular uptake of 30Kc19-HSA nanoparticles containing 0–70 wt% of 30Kc19 protein, which was measured using Alexa Fluor® 488-labeled nanoparticles. Human foreskin fibroblast was treated with nanoparticles for 24 h, and fluorescence was measured using a fluorometer. **b** Confocal microscopy image of human foreskin fibroblast treated with 200 μg/ml of 30Kc19-HSA nanoparticles containing 0–70 wt.% of 30Kc19 protein for 24 h. Nanoparticles were labeled with Alexa Fluor® 488 (green fluorescence), and nuclei were stained with Hoechst 33342 (*blue fluorescence*). **c** Lysosomal targeting of 50 % 30Kc19-HSA nanoparticles in human foreskin fibroblast. Nanoparticles were labeled with Alexa Fluor® 488 (*green fluorescence*), and lysosomes were labeled with LysoTracker (*red fluorescence*). *$p < 0.05$, compared with the control group ($n = 3$). *Error bars* represent standard deviation (Color figure online)

Cellular uptake of nanoparticles

Cellular uptake of 30Kc19-HSA nanoparticles containing α-galactosidase was assessed using fluorescent-labeled nanoparticles (Fig. 4a). 30Kc19-HSA nanoparticles exhibited higher cellular uptake into human foreskin fibroblast when compared with HSA nanoparticles. The fibroblast treated with 30 and 50 % 30Kc19-HSA nanoparticles for 24 h exhibited 1.5-fold higher fluorescence than HSA nanoparticle-treated cells. Nanoparticles with 70 % 30Kc19 protein showed small increase in cellular uptake than HSA nanoparticles.

Confocal microscope images of human fibroblast treated with nanoparticles were taken to assess uptake of nanoparticles in visual perspective (Fig. 4b). After 24-h treatment, higher fluorescence was observed in cells treated with nanoparticles containing 30Kc19 protein than with HSA-only nanoparticles. Fluorescence of HSA and 30Kc19-HSA nanoparticles was observed as a punctuate form in cytoplasmic area. To verify lysosomal localization of nanoparticles, nanoparticles with 50 % 30Kc19 were treated with LysoTracker (Fig. 4c). When merged, green fluorescence from nanoparticles and red fluorescence from LysoTracker were co-localized and presented as yellow dots, showing localization of 30Kc19-HSA nanoparticles in lysosomes.

Intracellular α-galactosidase activity delivered by nanoparticles

To investigate the α-galactosidase activity delivered directly or via protein nanoparticles, human foreskin fibroblast cells were treated with α-galactosidase, α-galactosidase-containing HSA nanoparticles, or α-galactosidase-containing 30Kc19-HSA nanoparticles for 24 h and the α-galactosidase activity of cell lysate was assayed using colorimetrical method (Fig. 5). Cells treated with α-galactosidase and α-galactosidase-containing HSA nanoparticles exhibited scarce intracellular α-galactosidase activity after 24 h. However, α-galactosidase delivered using 30Kc19-HSA nanoparticles retained enzyme activity even after 24 h. Fifty-percent 30Kc19-HSA nanoparticles exhibited the highest α-galactosidase activity.

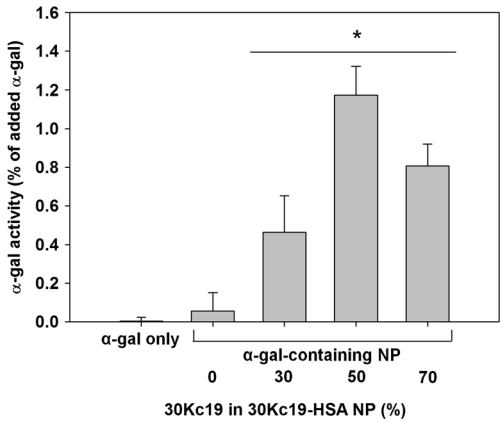

Fig. 5 Quantitative analysis of α-galactosidase activity in human foreskin fibroblast treated with 30Kc19-HSA nanoparticles containing α-galactosidase and 0–70 wt% of 30Kc19 protein. The α-galactosidase was added to the media at 4 μg/ml. Intracellular α-galactosidase activity was measured after 24-h incubation. *$p < 0.05$, compared with the control group ($n = 3$). *Error bars* represent standard deviation

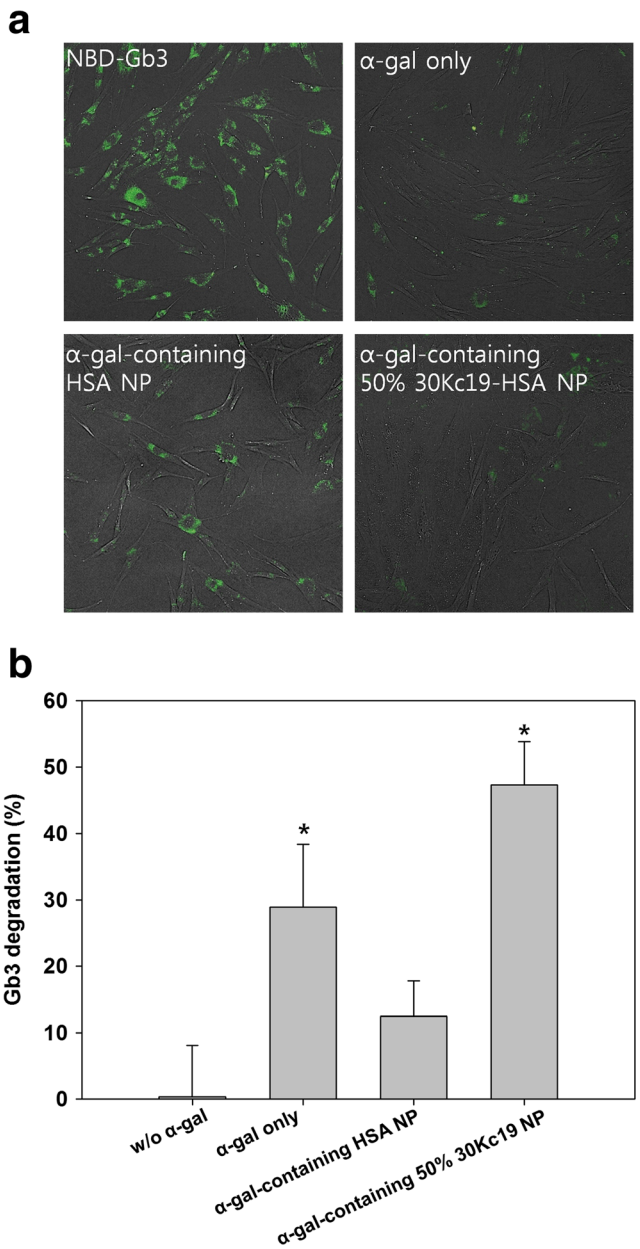

Fig. 6 Globotriaosylceramide degradation activity in nanoparticle-treated Fabry disease fibroblast. The fibroblasts from Fabry disease patients (pretreated with NBD-GB3) were treated with α-galactosidase, α-galactosidase-containing HSA nanoparticles, or α-galactosidase-containing 50 % 30Kc19 nanoparticles for 24 h. The α-galactosidase was added to the media at 4 μg/ml. **a** Fluorescence microscopy image of Fabry fibroblast treated with α-galactosidase only, α-galactosidase-containing HSA nanoparticles, or α-galactosidase-containing 50 % 30Kc19 nanoparticles. A *green fluorescence* represents remaining NBD-GB3. **b** Quantitative analysis of Gb3 degradation using fluorometer. *$p < 0.05$, compared with the control group ($n = 3$). *Error bars* represent standard deviation (Color figure online)

Globotriaosylceramide degradation activity in nanoparticle-treated Fabry disease fibroblast

The therapeutic efficiency of 30Kc19-HSA nanoparticles containing α-galactosidase was assessed using fibroblast from Fabry disease patients. Fabry fibroblast was pretreated with fluorescent Gb3 analog; then, α-galactosidase, α-galactosidase-containing HSA nanoparticles, and α-galactosidase-containing 50 % 30Kc19-HSA nanoparticles were added. Then, Gb3 degradation activity was visualized (Fig. 6a) and quantified using fluorometer (Fig. 6b). After 24 h, 29 % of initial NBD-GB3 was degraded in the α-galactosidase-treated cells, whereas α-galactosidase-containing HSA nanoparticles exhibited only 12 % NBD-GB3 degradation. Meanwhile, 50 % 30Kc19-HSA nanoparticles degraded 47 % of NBD-GB3, 3.8-fold higher than HSA nanoparticles and 1.6-fold higher than α-galactosidase itself.

Discussion

In this study, α-galactosidase was selected as the therapeutic cargo protein. We have demonstrated the effective role of the 30Kc19 for α-galactosidase-containing 30Kc19-HSA protein nanoparticles that can be used for the treatment of Fabry disease (Fig. 7). When 30Kc19 protein was applied in delivering actual drug as a nanocarrier, activity of therapeutic α-galactosidase was stabilized during the formation process of nanoparticles and also after the cellular uptake. The stabilization effect would be even more effective when applied in vivo because of degradation by proteases and immune reaction. Cellular uptake of α-galactosidase was also enhanced by cell-penetrating activity of 30Kc19, which is crucial for contemporary in vivo drug delivery. Therapeutic efficiency of 30Kc19-HSA nanoparticles containing α-galactosidase was assessed from Fabry disease patient-derived fibroblasts and showed almost 50 % decrease in NBD-Gb3 (Fig. 6). HSA has its own receptor-mediated endocytosis pathway, but α-galactosidase itself can internalize into cells and target lysosome via mannose 6-phosphate receptor, so it showed high uptake efficiency to cells and lysosomal targeting.

Most importantly, the cellular toxicity of 30Kc19-HSA nanoparticle containing α-galactosidase showed no significant change in the viability (Fig. 3). This is consistent with a previous study, which reported that it is non-toxic in vitro and in vivo (Park et al. 2012a) and that 30Kc19-HSA nanoparticles showed negligible toxicity in HeLa and HEK293 cells (Lee et al. 2014). Treatment of 30Kc19-HSA nanoparticles exhibited no toxicity on human primary cells and cell lines, suggesting that drug delivery using 30Kc19-HSA nanoparticles would be acceptable as drug delivery carrier for in vivo ERT.

Although 30Kc19 protein is beneficial, an area of improvement could be in increasing the amount making the protein nanoparticles. This is because it is limited by structural instability caused by increasing 30Kc19 content in nanoparticles (Lee et al. 2014). If nanoparticles can be formed using solely 30Kc19 protein with stable form, the beneficial effect of 30Kc19 in cargo uptake and stabilization could be maximized. The 30Kc19 protein consists of N-terminal domain α-helices and C-terminal domain β-sheets (Yang et al. 2011). According to our recent study, the 30Kc19 protein has a short cell-penetrating peptide at N-terminal domain (Park et al. 2014). We also recently produced soluble recombinant N-terminal domain α-helices of 30Kc19 and observed that it exhibited similar protein-stabilizing activity. Further study is required in order to investigate whether protein nanoparticles can be stably formed using only the N-terminal domain α-helices of 30Kc19 without HSA. Another area of improvement could be in reducing the size of protein nanoparticles, which would possibly increase the cellular uptake of therapeutic drugs.

Fluorescence of HSA and 30Kc19-HSA nanoparticles was observed as a punctuate form in cytoplasmic area, suggesting that nanoparticles were trapped in late endosome and lysosome (Fig. 4). Since α-galactosidase is a drug for the lysosomal storage disorder, lysosomal trafficking of 30Kc19-HSA nanoparticles could be suitable for a cellular α-galactosidase delivery. Possible future application could be to target potential lysosomal-related disorders.

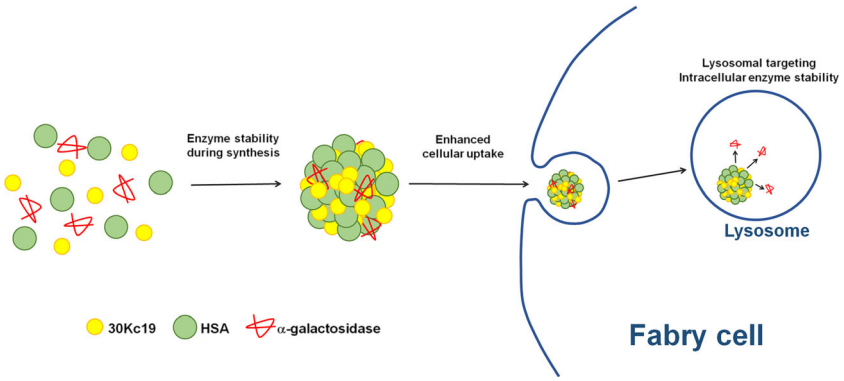

Fig. 7 A schematic illustration of α-galactosidase delivery by 30Kc19-human serum albumin (HSA) nanoparticles for the treatment of Fabry disease. Enhancement in cellular uptake and stabilization of α-galactosidase during the nanoparticle formation process and after the cellular uptake by 30Kc19 protein

Acknowledgments This study was supported by the National Research Foundation of Korea (NRF) funded by the Ministry of Science, ICT, & Future Planning (2015061592).

Compliance with ethical standards

Funding This study was funded by the Ministry of Science, ICT, and Future Planning (2015061592).

Conflict of interest The authors declare that they have no conflict of interest.

Ethical approval This article does not contain any studies with human participants or animals performed by any of the authors.

References

Azarmi S, Huang Y, Chen H, McQuarrie S, Abrams D, Roa W, Finlay WH, Miller GG, Löbenberg R (2006) Optimization of a two-step desolvation method for preparing gelatin nanoparticles and cell uptake studies in 143B osteosarcoma cancer cells. J Pharm Pharm Sci 9(1):124–132

Choi SS, Rhee WJ, Kim EJ, Park TH (2006) Enhancement of recombinant protein production in Chinese hamster ovary cells through anti-apoptosis engineering using *30Kc6* gene. Biotechnol Bioeng 95(3):459–467

Choi SS, Rhee WJ, Park TH (2002) Inhibition of human cell apoptosis by silkworm hemolymph. Biotechnol Prog 18(4):874–878

Choi SS, Rhee WJ, Park TH (2005) Beneficial effect of silkworm hemolymph on a CHO cell system: inhibition of apoptosis and increase of EPO production. Biotechnol Bioeng 91(7):793–800

Elzoghby AO, Samy WM, Elgindy NA (2012) Albumin-based nanoparticles as potential controlled release drug delivery systems. J Control Release 157(2):168–182

Ha S, Park T (1997) Efficient production of recombinant protein in *Spodoptera frugiperda*/AcNPV system utilizing silkworm hemolymph. Biotechnol Lett 19(11):1087–1091

Ha SH, Park TH, Kim S-E (1996) Silkworm hemolymph as a substitute for fetal bovine serum in insect cell culture. Biotechnol Tech 10(6):401–406

Irache J, Merodio M, Arnedo A, Camapanero M, Mirshahi M, Espuelas S (2005) Albumin nanoparticles for the intravitreal delivery of anticytomegaloviral drugs. Mini Rev Med Chem 5(3):293–305

Kim EJ, Park HJ, Park TH (2003) Inhibition of apoptosis by recombinant 30K protein originating from silkworm hemolymph. Biochem Biophys Res Commun 308(3):523–528

Kim EJ, Park TH (2003) Anti-apoptosis engineering. Biotechnol Bioprocess Eng 8(2):76–82

Kim EJ, Rhee WJ, Park TH (2004) Inhibition of apoptosis by a *Bombyx mori* gene. Biotechnol Prog 20(1):324–329

Kumar M (2000) Nano and microparticles as controlled drug delivery devices. J Pharm Pharm Sci 3(2):234–258

Lee HJ, Park HH, Kim JA, Park JH, Ryu J, Choi J, Lee J, Rhee WJ, Park TH (2014) Enzyme delivery using the 30Kc19 protein and human serum albumin nanoparticles. Biomaterials 35(5):1696–1704

Lee K, Jin X, Zhang K, Copertino L, Andrews L, Baker-Malcolm J, Geagan L, Qiu H, Seiger K, Barngrover D (2003) A biochemical and pharmacological comparison of enzyme replacement therapies for the glycolipid storage disorder Fabry disease. Glycobiology 13(4):305–313

Linthorst GE, Hollak CE, Donker-Koopman WE, Strijland A, Aerts JM (2004) Enzyme therapy for Fabry disease: neutralizing antibodies toward agalsidase alpha and beta. Kidney Int 66(4):1589–1595

Park HH, Choi J, Lee HJ, Ryu J, Park JH, Rhee WJ, Park TH (2015) Enhancement of human erythropoietin production in Chinese hamster ovary cells through supplementation of 30Kc19-30Kc6 fusion protein. Process Biochem 50(6):973–980

Park HH, Sohn Y, Yeo JW, Park JH, Lee HJ, Ryu J, Rhee WJ, Park TH (2014) Identification and characterization of a novel cell-penetrating peptide of 30Kc19 protein derived from *Bombyx mori*. Process Biochem 49(9):1516–1526

Park JH, Lee JH, Park HH, Rhee WJ, Choi SS, Park TH (2012a) A protein delivery system using 30Kc19 cell-penetrating protein originating from silkworm. Biomaterials 33(35):9127–9134

Park JH, Park HH, Choi SS, Park TH (2012b) Stabilization of enzymes by the recombinant 30Kc19 protein. Process Biochem 47(1):164–169

Rhee WJ, Kim EJ, Park TH (1999) Kinetic effect of silkworm hemolymph on the delayed host cell death in an insect cell-baculovirus system. Biotechnol Prog 15(6):1028–1032

Rhee WJ, Kim EJ, Park TH (2002) Silkworm hemolymph as a potent inhibitor of apoptosis in Sf9 cells. Biochem Biophys Res Commun 295(4):779–783

Rhee WJ, Park TH (2000) Silkworm hemolymph inhibits baculovirus-induced insect cell apoptosis. Biochem Biophys Res Commun 271(1):186–190

Scriver CR (2001) The metabolic & molecular bases of inherited disease, vol 4. McGraw-Hill, New York; Montreal

Vedder AC, Linthorst GE, Houge G, Groener JE, Ormel EE, Bouma BJ, Aerts JM, Hirth A, Hollak CE (2007) Treatment of Fabry disease: outcome of a comparative trial with agalsidase alfa or beta at a dose of 0.2 mg/kg. PLoS One 2(7):e598

von Storp B, Engel A, Boeker A, Ploeger M, Langer K (2012) Albumin nanoparticles with predictable size by desolvation procedure. J Microencapsul 29(2):138–146

Wang AZ, Gu F, Zhang L, Chan JM, Radovic-Moreno A, Shaikh MR, Farokhzad OC (2008) Biofunctionalized targeted nanoparticles for therapeutic applications. Expert Opin Biol Ther 8(8):1063–1070

Wang Z, Park JH, Park HH, Tan W, Park TH (2011) Enhancement of recombinant human EPO production and sialylation in Chinese hamster ovary cells through *Bombyx mori 30Kc19* gene expression. Biotechnol Bioeng 108(7):1634–1642

Weber C, Coester C, Kreuter J, Langer K (2000) Desolvation process and surface characterisation of protein nanoparticles. Int J Pharm 194(1): 91–102

Yang J-P, Ma X-X, He Y-X, Li W-F, Kang Y, Bao R, Chen Y, Zhou C-Z (2011) Crystal structure of the 30K protein from the silkworm *Bombyx mori* reveals a new member of the β-trefoil superfamily. J Struct Biol 175(1):97–103

Zensi A, Begley D, Pontikis C, Legros C, Mihoreanu L, Wagner S, Büchel C, von Briesen H, Kreuter J (2009) Albumin nanoparticles targeted with Apo E enter the CNS by transcytosis and are delivered to neurones. J Control Release 137(1):78–86